

Percolation Model for Relaxation in Random Systems

R. V. Chamberlin and D. N. Haines^(a)

Department of Physics, Arizona State University, Tempe, Arizona 85287-1504

(Received 22 March 1990)

We have measured the magnetic relaxation of several Au:Fe alloys from 10^{-5} to 10^4 sec after removing an applied field. The quality and range of the data are sufficient to demonstrate significant deviations from all functions previously used to characterize the dynamics of similar systems. A simple model, activated relaxation of dispersive excitations on a percolation distribution of finite-sized domains, gives excellent agreement with the measurements and may provide a common link between fundamental excitations and observed behavior in random systems.

PACS numbers: 75.50.Kj, 64.60.Ak

Some remarkably "universal" empirical functions have been used to characterize the dynamical behavior of a wide range of random systems.¹⁻³ Dilute magnetic alloys⁴ provide a canonical system by which these empirical functions may be tested. We have measured the magnetic relaxation of Au:Fe alloys with iron concentrations from 4% ("spin glass") through 21% ("random ferromagnet"). The quality and range of the data are sufficient to demonstrate significant deviations from all functions previously used to characterize the relaxation in similar systems.⁵⁻¹⁰ A simple model for magnon relaxation on a percolation distribution of finite domains gives excellent agreement with the observed behavior. Because the model is based on general geometric considerations, it is applicable to any random system with dispersive excitations, and may provide a physical basis for the universal aspects of dynamics in random systems.

Several investigators have previously considered the role of finite domains in the dynamics of random systems.¹¹⁻¹⁴ The primary distinction of our approach is that we consider only dispersive excitations within fixed finite domains; we find that local spin excitations, domain rotation, and wall motion need not be considered from 10^{-5} to 10^4 sec. We define a correlated domain as a region where excitations share a common dynamical phase factor, so that all spins within a domain have the same average level of excitation. Assuming linear response, the net relaxation is the probability that a given spin belongs to a domain containing s spins (sn_s), times the probability that this domain has not reached equilibrium, summed over all domains: $M(t) \propto \sum_s (sn_s) \times e^{-w_s t}$. The principal result of this Letter is that for relaxation rates which vary exponentially with inverse domain size ($w_s \propto e^{\pm c/s}$, characteristic of finite-size quantized dispersive excitations) these relaxation functions provide excellent agreement with observed behavior.

If a given spin is assumed to be correlated with at least one of its neighbors with probability p , percolation theory^{15,16} provides specific predictions for the distribution of finite domains. For $p > p_c$ (p_c is the critical probability for bond percolation) in three dimensions,^{17,18} ($sn_s) \propto s^{10/9} \exp[-(C's)^{2/3}]$, where $C' \propto |p - p_c|^{1/\sigma}$ and $\sigma = 0.45$. For activated relaxation of quantized systems

at temperature T ,¹⁹ $w_s \propto e^{-\delta E/k_B T}$. All dispersive excitations in finite systems have an average energy-level spacing (δE) which is inversely proportional to the number of particles in the system.^{20,21} This is simply a statement that since s discrete levels fill a fixed bandwidth, $\delta E = \Delta/s$ (Δ depends only on the average interaction between spins, independent of domain size). Using $x = C's$, the net relaxation becomes

$$M(t) = M_i \int_0^\infty x^{10/9} \exp(-x^{2/3}) \exp(-tw - e^{-C/x}) dx, \quad (1)$$

where the adjustable parameters are $C = C'\Delta/k_B T$, the initial response $[3\Gamma(\frac{19}{6})/2]M_i = 3.518M_i$, and w_- the relaxation rate for the largest finite domain (smaller domains have larger energy-level spacing and hence relax more slowly). Although the average-sized domains [$\bar{x} = (\frac{19}{6})^{3/2}$] produce the predominant behavior, for $C \gg 1$ the spectrum is extremely broad.

The phase diagram of Au:Fe includes several random magnetic phases.²² All concentrations we have measured show qualitatively similar relaxational behavior. Here we focus on three samples: SG8 (8.0% Fe) exhibited a spin-glass-like cusp at $T_g = 28$ K; CG12 (11.9% Fe) had a sharp maximum at $T_m = 39$ K (characteristic of a concentrated spin glass); whereas the field-cooled magnetization of RF20 (19.8% Fe) was featureless throughout its random-ferromagnetic regimes. Relaxation of the thermoremanent magnetization was measured using a SQUID magnetometer coupled to a high-speed voltmeter. A magnetic field ($H = 3.6$ Oe) was applied to the sample while at an elevated temperature. The sample was then field cooled to the measurement temperature. After a specified wait time ($t_w \sim 10^3$ sec), H was removed and the magnetization recorded as a function of time. Data were taken at 10- μ sec intervals from the moment H was removed, and at increasing intervals until 10^2 - 10^4 sec. The absolute magnetization was determined before and after each relaxation by moving the sample between two counterwound coils.

The magnetic relaxation of CG12 at three temperatures above T_m is shown in Fig. 1. The solid curves are the best fits using Eq. (1) over the range 10^{-4} - 10^1 sec. The inset shows the deviations of the data from these fits.

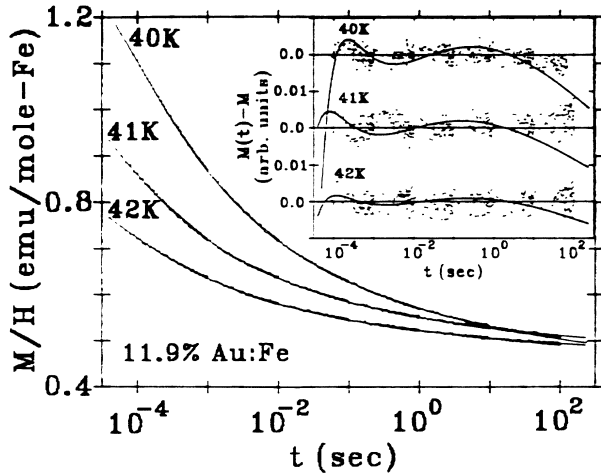


FIG. 1. Magnetic relaxation of sample CG12 at three temperatures above the transition $T_m = 39$ K. The solid curves are the best fits using Eq. (1) over the range 10^{-4} - 10^1 sec. Extrapolation to shorter and longer times reveals no systematic deviation. Inset: Difference between Eq. (1) and the data. The best fits by a simple power law (solid curves) are shown for comparison.

For comparison, the best fits using a simple power law (solid curves) are also shown. The validity of Eq. (1) is confirmed by the fact that no systematic deviations are observed, and that fitting over a reduced time range produces curves which extrapolate through the data at longer and shorter times. Although it is difficult to experimentally determine the precise distribution of finite domains, the distribution for $p < p_c$ invariably gives inferior results, suggesting that the dynamical correlation length is sufficiently long ranged to produce percolation, even in dilute samples above their transition. The spin waves in each finite domain are quantized with energy-level spacing inversely proportional to the number of spins. In the field-cooled state, the induced magnetic moment of each domain is aligned with the field. When H is removed the average internal energy of the domains must increase from the field-cooled state to the zero-field equilibrium. The quality of the fits indicates that other relaxation mechanisms need not be considered.

The magnetic relaxation of CG12 at four temperatures below T_m (Fig. 2) shows two distinct regimes of relaxation. It is natural to assume that there may also be domains whose average internal energy must decrease from the field-cooled state to the zero-field equilibrium:

$$M(t) = M_i \int_0^\infty x^{10/9} \exp(-x^{2/3}) \exp(-tw + e^{+C/x}) dx. \tag{2}$$

Here w_+ is the slowest relaxation rate (the larger energy-level spacing of smaller domains expedites energy loss). This relaxation may be due to domains with pure antiferromagnetic order, or domains whose induced magnetic moment was antialigned with H . At present we

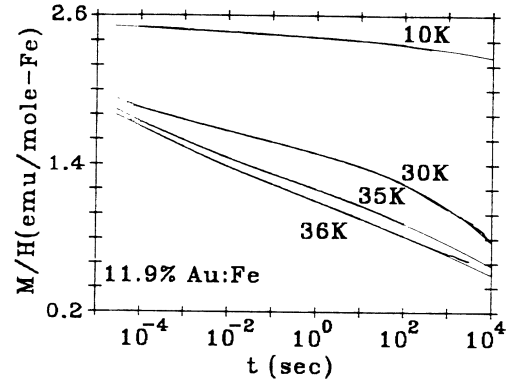


FIG. 2. Magnetic relaxation of sample CG12 at four temperatures below $T_m = 39$ K. The solid curves are the best fits using Eq. (1) plus Eq. (2) over the range 10^{-4} - 10^2 sec.

favor the antialigned picture since experimentally these domains have similar energy-level spacing and size distribution. Least-squares fits by Eq. (1) plus Eq. (2) from 10^{-4} to 10^2 sec (solid curves in Fig. 2) show excellent agreement over the fit range and generally extrapolate through the data at longer and shorter times. The dominant source of deviation at long times is instrument drift; however, some systematic slowing for $t > t_w$ is also observed. For $t < t_w$, increasing t_w produces a decrease in C , confirming that waiting-time effects²³⁻²⁵ may be due to domain growth in the field-cooled state.²⁶

The magnetic relaxation of sample RF20 at 40 K is shown in Fig. 3. This relaxation exhibits several complex features which are accurately reproduced by Eqs. (1) and (2) (plus a constant base line necessary for this more concentrated sample). Little relaxation occurs before $1/w_- = 30$ μ sec. The locally steepest slope near $1/\bar{w}_- = 5$ msec [$\bar{w}_\pm \equiv w_\pm \exp(\pm C/\bar{x})$] is due to the relaxation of the average-sized aligned domains. At $1/\bar{w}_+$

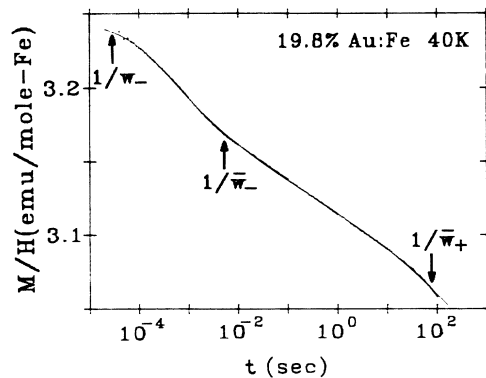


FIG. 3. Magnetic relaxation of sample RF20 at 40 K. The solid curve is the best fit using Eqs. (1) and (2). The complex relaxational behavior is due to the relaxation rates of the average-sized aligned ($1/\bar{w}_- = 5$ msec) and antialigned ($1/\bar{w}_+ = 80$ sec) domains, and the broad distribution from $1/w_- = 30$ μ sec to $1/w_+ = 10$ ksec.

=80 sec the magnetization again decreases more rapidly as the average-sized antialigned domains begin to relax. Negligible deviation between the fit and this complex behavior demonstrates the extreme accuracy of the percolation model.

The relaxation rates of the average-sized domains for SG8 and CG12 are shown in Fig. 4(a). Other physical quantities such as the correlation length (ξ), initial thermoremanent magnetization *per spin* (M_0), and magnon bandwidth (Δ) cannot be isolated from Eqs. (1) and (2) because they are coupled by integration over the dummy variable x . However, relative temperature dependences may be obtained by using $M_0 \propto M_i (\Delta/CT)^{\tau-2}$ and $\xi \propto (\Delta/CT)^{\sigma\nu}$ (where $\tau=2.2$, $\sigma=0.45$, and $\nu=0.88$ are percolation scaling exponents). For the physically reasonable assumption of constant bandwidth, M_0 and χ exhibit appealingly simple temperature behavior. The initial thermoremanent magnetization per spin [Fig. 4(b)] decreases linearly up to the transition, indicating a constant average energy-level spacing throughout this regime. Extrapolation to zero magnetization (solid lines) gives the temperature at which all magnons would be ac-

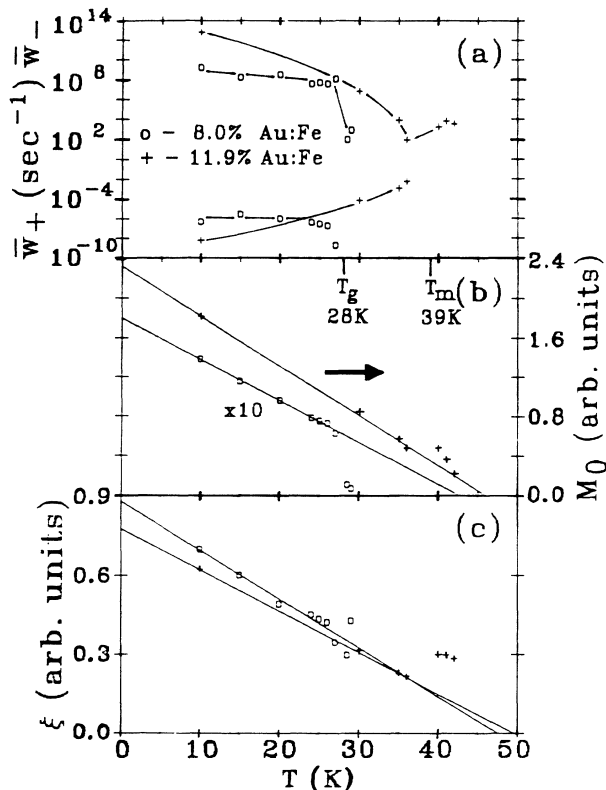


FIG. 4. (a) Temperature dependences of the average-sized aligned (\bar{w}_- , upper) and antialigned (\bar{w}_+ , lower) relaxation rates for SG8 (O) and CG12 (+); solid curves are guides for the eye. Relative temperature dependences of (b) the initial thermoremanent magnetization per spin (M_0) and (c) the correlation length (ξ) for these samples. Solid lines are the best fits by the linear regimes below $T_g=28\text{K}$ and $T_m=39\text{K}$.

tivated, providing an estimate for Δ ; we find 43 ± 2 and $46 \pm 2\text{K}$ for SG8 and CG12, respectively. Extrapolation to zero temperature provides a relative measure of the saturation magnetization. The strong concentration dependence indicates significant randomness in the ground state of dilute domains. The correlation lengths [Fig. 4(c)] are a minimum at the transition (in contrast to a divergence if this were a percolation transition). Below the transition ξ also decreases linearly with increasing temperature, extrapolating to zero at 47 ± 4 and $49 \pm 2\text{K}$ for SG8 and CG12, respectively.

Dilute Au:Fe was the first random system to exhibit a sharp susceptibility cusp,²⁷ initiating interest in the possibility of a spin-glass transition. Indeed, some thermodynamic transition may occur on the infinite backbone, but the accuracy of Eqs. (1) and (2) indicate that finite domains dominate the relaxational behavior. Above T_g , Eq. (1) implies that all domains are aligned with the magnetic field. In the vicinity of T_g , half the domains become antialigned. This picture is supported by the fact that spectra in the vicinity of the transition (27.5 and 28 K in SG8 and 37.5 and 39 K in CG12) could only be fitted using unequal fractions of aligned and antialigned domains, suggesting a 5%-10% "transition" width. Below T_g , Eqs. (1) and (2) indicate a well-defined energy-level distribution within each domain; randomness comes from size and orientational degeneracies. An applied field *increases* the internal energy of antialigned domains; they are frustrated from aligning with the field by interdomain interactions.

Various mathematical approximations to Eqs. (1) and (2) reproduce several of the empirical functions previously used to characterize relaxation in random systems. Converting Eq. (1) or (2) to an integration over relaxation times, to second order in the exponent about its maximum, gives a log-normal distribution.²⁸ Using a steepest-descent method valid for $Cw-t \gg 1$, Eq. (1) becomes a simple power law $M(t) \sim t^{-\alpha}$.²⁹ A similar approximation for Eq. (2) (valid when $Cw+t \lesssim 1$) reproduces the Kohlrausch-Williams-Watts stretched exponential $M(t) \sim \exp(-t^\beta)$.³⁰ Indeed, the best previously proposed functions invariably involve a power law and stretched exponential. For instance, the product^{6,7} $M(t) \sim t^{-\alpha} \exp[-(t/\tau)^\beta]$ [which has the same number of adjustable parameters as Eqs. (1) and (2)] gives χ_e^2 values yielding $\ln(\chi_e^2/\chi^2)$ of 0.18 ± 0.09 , -0.06 ± 0.11 , and 1.02 ± 0.13 for samples SG8, CG12, and RF20, respectively. Although both significant differences favor Eqs. (1) and (2), it is the simplicity of the model that is most appealing. Previous theoretical expressions do not fit as well; for example,¹⁴ $M(t) \sim [\ln(t)]^{-\theta/\psi}$ has $d^2M/d(\ln t)^2 > 0$, which is not observed for $t < t_w$ at low temperatures in either SG8 or CG12.

In conclusion, a simple model for relaxation of dispersive excitations on a percolation distribution of finite domains yields two mesoscopically exact relaxation functions. Various mathematical approximations to these

functions reproduce many of the empirical functions previously used to characterize dynamics in random systems. Magnetic relaxation measurements of Au:Fe demonstrate significant deviations from the empirical functions, but show excellent agreement with our percolation model. The model is not a microscopic theory, but may provide a common link between fundamental excitations and observed behavior. Indeed, stress relaxation in ionic glasses³¹ and dielectric susceptibility of glass-forming liquids³² also demonstrate significant deviations from all previously proposed relaxation functions, but show excellent agreement with our model.³³

Important contributions of P. M. Chaikin, G. S. Grest, S. M. Lindsay, R. F. Marzke, R. Orbach, O. F. Sankey, K. E. Schmidt, and G. H. Wolf are gratefully acknowledged. This research was supported by ONR Contract No. N00014-88-K-0094.

^(a)Present address: Department of Physics, University of Alabama, Huntsville, AL 35899.

- ¹J. Friedrich and A. Blumen, *Phys. Rev. B* **32**, 1434 (1985).
²M. F. Shlesinger and E. W. Montroll, *Proc. Natl. Acad. Sci. U.S.A.* **81**, 1280 (1984).
³K. L. Ngai, *Comments Solid State Phys.* **9**, 127 (1979); **9**, 141 (1979).
⁴For a review, see, K. Binder and A. P. Young, *Rev. Mod. Phys.* **58**, 801 (1986).
⁵R. V. Chamberlin, G. Mozurkewich, and R. Orbach, *Phys. Rev. Lett.* **52**, 867 (1984).
⁶A. T. Ogielski, *Phys. Rev. B* **32**, 7384 (1985).
⁷M. Alba, M. Ocio, and J. Hammann, *Europhys. Lett.* **2**, 45 (1986).
⁸J. L. van Hemmen and G. J. Nieuwenhuys, *Europhys. Lett.* **2**, 797 (1986).
⁹D. H. Reich, T. F. Rosenbaum, and G. Aeppli, *Phys. Rev. Lett.* **59**, 1969 (1987).

- ¹⁰N. Bontemps and R. Orbach, *Phys. Rev. B* **37**, 4708 (1988).
¹¹D. A. Smith, *J. Phys. F* **5**, 2148 (1975).
¹²K. Binder, *Z. Phys. B* **26**, 339 (1977).
¹³A. P. Malozemoff and E. Pytte, *Phys. Rev. B* **34**, 6579 (1986).
¹⁴D. S. Fisher and D. A. Huse, *Phys. Rev. Lett.* **56**, 1601 (1986); *Phys. Rev. B* **38**, 373 (1988).
¹⁵J. W. Essam, *Rep. Prog. Phys.* **43**, 833 (1980).
¹⁶D. Stauffer, A. Caniglio, and M. Adam, *Adv. Polym. Sci.* **44**, 103 (1982); D. Stauffer, *Introduction to Percolation Theory* (Taylor & Francis, Philadelphia, 1985).
¹⁷H. Kunz and B. Souillard, *Phys. Rev. Lett.* **40**, 133 (1978).
¹⁸T. C. Lubensky and A. J. McKane, *J. Phys. A* **14**, L157 (1981).
¹⁹P. Hänggi and H. Thomas, *Phys. Rep.* **88**, 207 (1982).
²⁰H. Fröhlich, *Physica (Utrecht)* **4**, 406 (1937).
²¹R. Kubo, *J. Phys. Soc. Jpn.* **17**, 975 (1962).
²²B. V. B. Sarkissian, *J. Phys. F* **11**, 2191 (1981).
²³L. Lundgren, P. Svedlindh, P. Nordblad, and O. Beckman, *Phys. Rev. Lett.* **51**, 911 (1983).
²⁴R. V. Chamberlin, *Phys. Rev. B* **30**, 5393 (1984).
²⁵P. Svedlindh, P. Granberg, P. Nordblad, L. Lundgren, and H. S. Chen, *Phys. Rev. B* **35**, 268 (1987).
²⁶G. Koper and H. Hilhorst, *J. Phys. (Paris)* **49**, 429 (1988).
²⁷V. Cannella, J. A. Mydosh, and J. I. Budnick, *J. Appl. Phys.* **42**, 1689 (1971).
²⁸Distribution of relaxation times $D_\tau \sim \exp[28(\ln W)/9 - W^{2/3}]/\tau$, where $W = \mp C/\ln(w \pm \tau)$.
²⁹Power-law exponent $\alpha \sim \bar{x}'[19 - 6(\bar{x}')^{2/3}]/9C$, where \bar{x}' is a time-averaged average-sized domain.
³⁰Stretched exponential exponent $\beta = 2/(5 + 3C/\bar{x}')$.
³¹R. Böhmer, H. Senapati, and C. A. Angell, in *Proceedings of the International Discussion Meeting on Relaxation in Complex Systems*, Crete, Greece, 1990 [*J. Non-Cryst. Solids* (to be published)].
³²P. K. Dixon, L. Wu, S. R. Nagel, B. D. Williams, and J. P. Carini, in *Proceedings of the International Discussion Meeting* (Ref. 31); *Phys. Rev. Lett.* **65**, 1108 (1990).
³³R. V. Chamberlin (to be published).